

Determination and correlation of infinite dilution binary diffusion coefficients for aluminum acetylacetonate in supercritical and liquid fluids

メタデータ	言語: eng 出版者: 公開日: 2018-07-26 キーワード (Ja): キーワード (En): 作成者: Kong, Chang Yi, Watanabe, Kou, Funazukuri, Toshitaka メールアドレス: 所属:
URL	http://hdl.handle.net/10297/00025585

Determination and correlation of infinite dilution binary diffusion coefficients for aluminum acetylacetonate in supercritical and liquid fluids

Chang Yi Kong^{1,2*}, Kou Watanabe¹, Toshitaka Funazukuri³

¹ Department of Engineering, Graduate School of Integrated Science and Technology, Shizuoka University, 3-5-1 Johoku Naka-ku, Hamamatsu 432-8561, Japan

² Research Institute of Green Science and Technology, Shizuoka University, 3-5-1 Johoku Naka-ku, Hamamatsu 432-8561, Japan

³ Department of Applied Chemistry, Faculty of Science and Engineering, Chuo University 1-13-27 Kasuga, Bunkyo-ku, Tokyo, 112-8551, Japan

* Corresponding author.

E-mail address: kong.changyi@shizuoka.ac.jp (C.Y. Kong).

Abstract

The infinite dilution binary diffusion coefficients D_{12} for aluminum acetylacetonate in supercritical CO₂ were determined at 308.15 – 333.15 K and at 7.80 to 40.00 MPa by the chromatographic impulse response (CIR) method. And, the diffusion measurements in liquid ethanol were carried out at 300.15 – 333.15 K and at 0.10 and 30.00 MPa by the Taylor dispersion method. It was found that the D_{12} values measured in supercritical CO₂ show slowing down in the region of near critical point. The determined activation energies of diffusion were 23.0, 13.7, 12.0, 11.3 kJ/mol at 12.00, 20.00, 25.00, 35.00 MPa in supercritical CO₂ and 19.1 kJ/mol at 0.10 MPa in liquid ethanol, respectively. All determined 90 diffusion data in this study can be correlated with the equation of $D_{12} [\text{m}^2/\text{s}] = 1.558 \times 10^{-14} T [\text{K}] \eta [\text{Pa s}]^{-0.761}$ with average absolute relative deviation (AARD) of 5.6% over a wide fluid viscosity range from 2.462×10^{-5} to 1.258×10^{-3} Pa s.

Key words: Diffusion coefficient, supercritical carbon dioxide, liquid, aluminum acetylacetonate, chromatographic impulse response

33 **1. Introduction**

34 Supercritical fluids as green solvents are now being often used in chemical reaction,
35 extraction, separation and analysis in both academia and industry thanks to unique properties
36 like high diffusivity, low kinetic viscosity and easily adjustable solvent power. For rational
37 design and improvement of the process with supercritical fluids, it is important to fully know
38 basic property such as the diffusion of solutes in the supercritical system. Diffusion is a
39 physical phenomenon commonly occurring in a variety of chemical, biological and
40 environmental processes involving mass transfer. Therefore, the determination of diffusivities
41 in fluids is of great significance for the estimation of mass transfer processes. A more efficient
42 application using supercritical fluid technology often adds entrainer to the supercritical fluid.
43 Hence the diffusion mechanisms in practical processes need to be understood not only in
44 supercritical state but also in liquid state. Up to now, most measurements of diffusion
45 coefficients relate only to liquid state or supercritical state. Furthermore, there is a lack of
46 diffusion data for the same solute in both states. There are many methods [1-3] that may be
47 used to obtain infinite dilution binary diffusion coefficients D_{12} . Among them, the Taylor
48 dispersion method is suitable for determining the D_{12} data in liquid phase, and the
49 chromatographic impulse response (CIR) method [4,5] can be used not only for measuring
50 diffusion but also for measuring partial molar volumes and solubilities in supercritical fluids
51 [6,7].

52 Aluminum acetylacetonate ($\text{Al}(\text{acac})_3$) as one of aluminum source can be soluble in
53 supercritical CO_2 . Through thermal decomposition in supercritical CO_2 , $\text{Al}(\text{acac})_3$ can be used
54 as a precursor to produce template nanoporous alumina materials [8], thin films of aluminum
55 oxide [9,10] and many important applications [11]. Diffusion data are still inconveniently few
56 for metal complexes [12-17] in supercritical CO_2 , and it is found that no diffusion data are
57 available for system of $\text{Al}(\text{acac})_3$ in supercritical CO_2 or in liquid ethanol. Therefore, this

58 study was intended to measure the D_{12} values for Al(acac)₃ in supercritical CO₂. In addition,
 59 the D_{12} data were also determined in liquid ethanol. Then, the reliability of the correlation of
 60 D_{12}/T vs fluid viscosity η was examined.

61

62 2. Theory

63 The detail theoretical backgrounds have been given by the authors [5] for the CIR method
 64 and Alizadeh et al. [18] for the Taylor dispersion method. The cross sectional average
 65 concentrations $c(z,t)$ can be given by using Eq. (1) for the CIR method and Eq. (2) for the
 66 Taylor dispersion method, respectively.

$$67 \begin{cases} c(z,t) = \left(\frac{m}{\pi R^2} \right) \left(\frac{u}{u_0} \right) \frac{1}{\sqrt{4\pi Kt}} \exp \left[-\frac{(z-ut)^2}{4Kt} \right] \\ K = \left[D_{12} + \frac{R^2}{48D_{12}} (6u^2 - 16u_0u + 11u_0^2) \right] \left(\frac{u}{u_0} \right) \end{cases} \quad (1)$$

$$68 \begin{cases} c(z,t) = \left(\frac{m}{\pi R^2} \right) \frac{1}{\sqrt{4\pi Kt}} \exp \left[-\frac{(z-u_0t)^2}{4Kt} \right] \\ K = D_{12} + \frac{R^2}{48D_{12}} u_0^2 \end{cases} \quad (2)$$

69 where z is the axial distance, t is the time, m is the amount injected, R is the column radius,
 70 u and u_0 are the solute and fluid velocities, respectively. The D_{12} was determined by curve
 71 fit using the root mean square fitting error ε (Eq. (3)). It was found that the fit indicated
 72 acceptably if $\varepsilon < 3\%$ and good if $\varepsilon < 1\%$ [5].

$$73 \varepsilon = \left(\frac{\int_{t_1}^{t_2} (c_{\text{meas}}(L,t) - c(L,t))^2 dt}{\int_{t_1}^{t_2} (c_{\text{meas}}(L,t))^2 dt} \right)^{1/2} \quad (3)$$

74 where L is the distance between injector and detector, t_1 and t_2 are the times at the frontal and
 75 latter 10% peak heights of measured curve $c_{\text{meas}}(L,t)$ at $z=L$, respectively.

76

77 3. Experimental

78 The measurement system basically consisted of a pump, a pressure gauge, an injector, a

79 diffusion column, a water bath, a thermometer, a UV-Vis multidetector and a back pressure
80 regulator. The apparatus and procedure have been described elsewhere [15-17]. The
81 measurements in this study were carried out at higher pressures, therefore, a high degree of
82 accuracy in both temperature and pressure control was desirable. The pulseless syringe pump
83 was used to supply compressed CO₂ in the CIR method, which can eliminate pressure and
84 density gradients in supercritical CO₂. Note that in this study the pressure and temperature
85 were controlled accurately to ±0.01 K and ±0.05 bar, respectively. Then, a pulse of Al(acac)₃
86 dissolved in hexane or ethanol was loaded through the injector. When the solute was injected,
87 the injection mode must be carefully checked. If the sample rotor was left in the flowing fluid,
88 the measured response curve with serious tailing was often gotten. But, after injected with a
89 very short time (e.g. less than 1 s), then the injection valve being immediately turned to allow
90 the fluid to flow directly to the column, it often got in a pulse like injection, the tailing may be
91 avoided and the dispersion effect of the solute was minimally-eliminated. The
92 chromatographic response curves were measured by the UV detector with 1 nm increments.

93 CO₂ with purity of 99.95% was purchased from Air Gases Tokai Ltd., Japan, aluminum
94 acetylacetonate (molecular formula: Al(C₅H₇O₂)₃, molecular weight: 324.3) with 99% was
95 obtained from Sigma Aldrich, ethanol with 99.5% was from Wako, hexane with 98% was
96 obtained from Tokyo Chemical Industry, and all materials used as received.

97

98 **4. Results and discussion**

99 We have examined the effects of the injected Al(acac)₃ concentration, the wavelength, the
100 fluid velocity and the dissolving organic solvent on D_{12} of Al(acac)₃ as described elsewhere
101 [17,19]. The Al(acac)₃ concentration of ethanol with 7.5×10^{-4} g/mL and the wavelength of
102 300 nm were used in all diffusion measurements. The fluid velocities were controlled at lower
103 than 8×10^{-3} m/s, and all measurements were made at $DeSc^{1/2} < 8$, where De is the Dean

104 number and Sc is the Schmidt number. In this study at least three measurements at the given
 105 condition were measured, and the average diffusion datum was determined to be the D_{12} value.
 106 All determined D_{12} data are presented in Table 1, together with the values of fluid density ρ
 107 and viscosity η .
 108

Table 1

Infinite dilution binary diffusion coefficient D_{12} data of $\text{Al}(\text{acac})_3$ measured in supercritical CO_2 at 308.15 to 333.15 K and in liquid ethanol at 300.15 to 333.15 K, together with the densities ρ and viscosities η of the fluids.

P (MPa)	ρ (kg/m ³)	η (10 ⁻⁶ Pa s)	D_{12} (10 ⁻⁸ m ² /s)
<i>Measured by the CIR method in supercritical CO₂</i>			
308.15 (K)			
7.80	331.50	24.62	1.163
7.95	388.81	28.15	1.096
8.00	419.09	30.17	1.072
8.05	455.61	32.54	1.028
8.10	490.76	34.95	1.004
8.20	542.80	39.26	1.004
8.30	574.13	42.12	1.045
8.40	595.70	44.21	1.045
8.50	612.12	45.87	0.992
8.80	646.10	49.52	0.964
9.00	662.13	51.36	0.926
9.50	691.50	54.92	0.882
10.00	712.81	57.68	0.840
10.50	729.76	60.00	0.802
11.00	743.95	62.03	0.788
12.00	767.07	65.51	0.754
13.00	785.70	68.50	0.718
14.00	801.41	71.15	0.709
16.00	827.17	75.81	0.667
18.00	848.04	79.88	0.620
20.00	865.72	83.56	0.607
22.00	881.15	86.97	0.593

23.00	888.20	88.59	0.573
24.00	894.88	90.16	0.571
25.00	901.23	91.69	0.564
30.00	929.11	98.86	0.518
32.00	938.84	101.54	0.515
35.00	952.29	105.42	0.505
40.00	972.26	111.57	0.480

313.15 (K)

8.40	334.71	25.02	1.447
8.50	353.91	26.06	1.398
8.60	375.95	27.33	1.321
8.70	401.13	28.87	1.273
8.80	429.10	30.70	1.216
8.90	458.03	32.72	1.121
9.00	485.50	34.77	1.145
9.10	510.38	36.75	1.109
9.30	550.54	40.17	1.114
9.50	580.01	42.90	1.055
10.00	628.61	47.81	0.984
10.50	660.15	51.33	0.944
11.00	683.52	54.11	0.925
11.50	702.18	56.46	0.872
12.00	717.76	58.52	0.846
13.00	743.04	62.05	0.797
15.00	780.23	67.73	0.746
16.00	794.90	70.16	0.718
17.00	807.87	72.39	0.701
19.00	830.09	76.45	0.675
20.00	839.81	78.32	0.657
21.00	848.81	80.10	0.646
25.00	879.49	86.62	0.598
30.00	909.89	93.83	0.561
32.00	920.39	96.51	0.543
35.00	934.81	100.37	0.534
40.00	956.07	106.46	0.499

323.15 (K)

9.80	361.28	26.98	1.498
10.00	384.33	28.33	1.457
10.10	396.32	29.06	1.392
10.30	420.88	30.64	1.344
10.50	445.55	32.32	1.250
10.80	480.95	34.90	1.256
11.00	502.64	36.59	1.245
11.50	548.84	40.48	1.176
12.00	584.71	43.79	1.144
13.00	636.12	49.04	1.063
15.00	699.75	56.52	0.933
18.00	757.12	64.44	0.838
20.00	784.29	68.67	0.780
22.00	806.61	72.41	0.751
25.00	834.19	77.42	0.710
30.00	870.43	84.75	0.657
35.00	899.23	91.27	0.619

333.15 (K)

12.00	434.43	32.02	1.460
13.00	505.35	37.27	1.326
14.00	561.37	42.05	1.220
15.00	604.09	46.13	1.128
16.00	637.50	49.61	1.092
18.00	687.25	55.35	0.996
20.00	723.68	60.04	0.904
22.00	752.38	64.07	0.852
25.00	786.55	69.33	0.792
30.00	829.71	76.82	0.739
35.00	862.94	83.34	0.699

Measured by the Taylor dispersion method in liquid ethanol

300.15 (K)

0.10	783.79	1071.12	0.073
30.00	807.52	1258.39	0.063

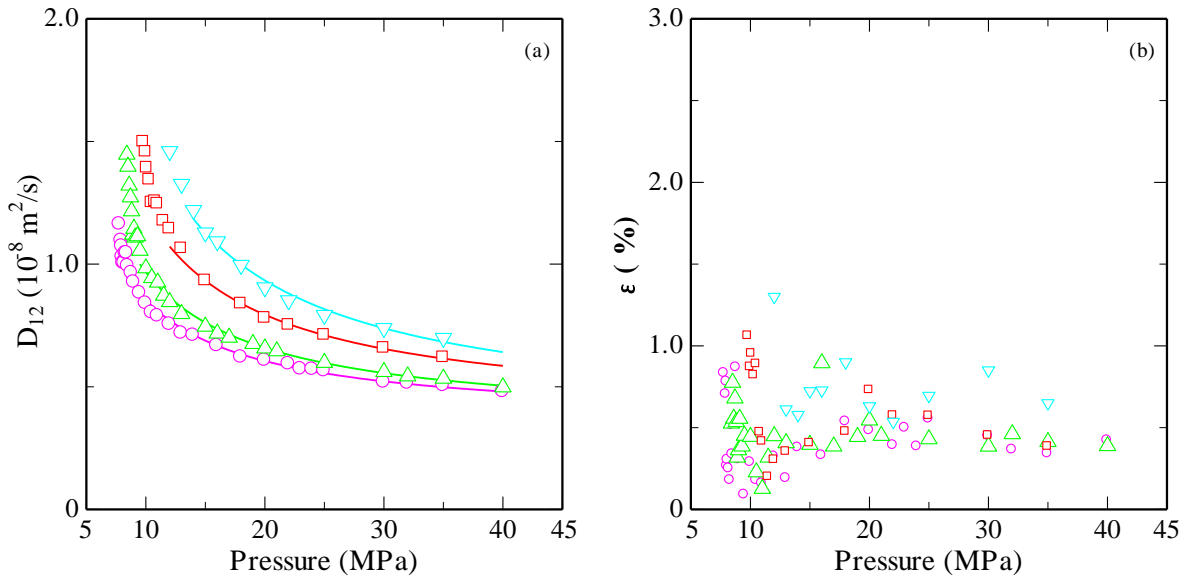
313.15 (K)

0.10	772.56	844.89	0.106
30.00	797.97	1003.37	0.089
323.15 (K)			
0.10	763.62	711.01	0.126
333.15 (K)			
0.10	754.36	602.99	0.157

109 ^a Standard uncertainties are 0.02 K for $u(T)$, 0.01 MPa for $u(P)$. The combined expanded
 110 uncertainty $U_c(D_{12})$ is 4×10^{-13} m²/s at 0.95 level of confidence with $k=2$.

111

112



113

114 Fig. 1. Pressure dependence on the (a) D_{12} and (b) ε of $\text{Al}(\text{acac})_3$ measured at 308.15 K (\circ),
 115 313.15 K (\triangle), 323.15 K (\square) and 333.15 K (∇), and at 7.80 to 40.00 MPa in supercritical CO_2
 116 by the CIR method, and together with the correlated line (with best AARD%) by Eq. (4).

117

118 Fig. 1 illustrates the pressure influence on the determined D_{12} and ε by the CIR method
 119 for $\text{Al}(\text{acac})_3$ at 308.15, 313.15, 323.15 and 333.15 K, and pressures from 7.80 to 40.00 MPa
 120 in supercritical CO_2 . Almost ε values were lower than 1% as seen in Fig. 1 (b). The greater
 121 pressure sensitivity of D_{12} at lower pressure indicates that the fluid density or viscosity is
 122 remarkable factor, because these properties change rapidly with pressure in this region. It was

123 found that an empirical correlation (Eq. (4)) can represent the 84 D_{12} data for $\text{Al}(\text{acac})_3$
 124 determined in supercritical CO_2 with the average absolute relative deviation (AARD) of 3.9%.

$$125 \quad D_{12} = c_0 + c_1 \frac{1}{P} + c_2 T + c_3 \frac{T}{P} \quad (4)$$

$$126 \quad \text{AARD} = \frac{1}{N} \sum_{i=1}^N \left| \frac{D_{12,\text{meas}} - D_{12,\text{pred}}}{D_{12,\text{meas}}} \right|_i \times 100\% \quad (5)$$

127 where D_{12} , c_0 , c_1 , c_2 , c_3 , T and P are in m^2/s , m^2/s , $\text{m}^2 \text{MPa}/\text{s}$, $\text{m}^2/(\text{s K})$, $\text{m}^2 \text{MPa}/(\text{s K})$, K and
 128 MPa, respectively, N is the number of experimental data points, and $D_{12,\text{meas}}$ and $D_{12,\text{pred}}$ are
 129 the measured and predicted D_{12} data, respectively. The parameters of c_0 to c_3 determined
 130 individual fittings at 308.15, 313.15, 323.15 and 333.15 K and a global fitting are presented in
 131 Table 2 with the values of N and AARD. It was found [12,14,17,20] that the simple empirical
 132 correlation can well represent the D_{12} data determined in this study over the higher pressure
 133 region, as shown in Fig. 1 and Table 2.

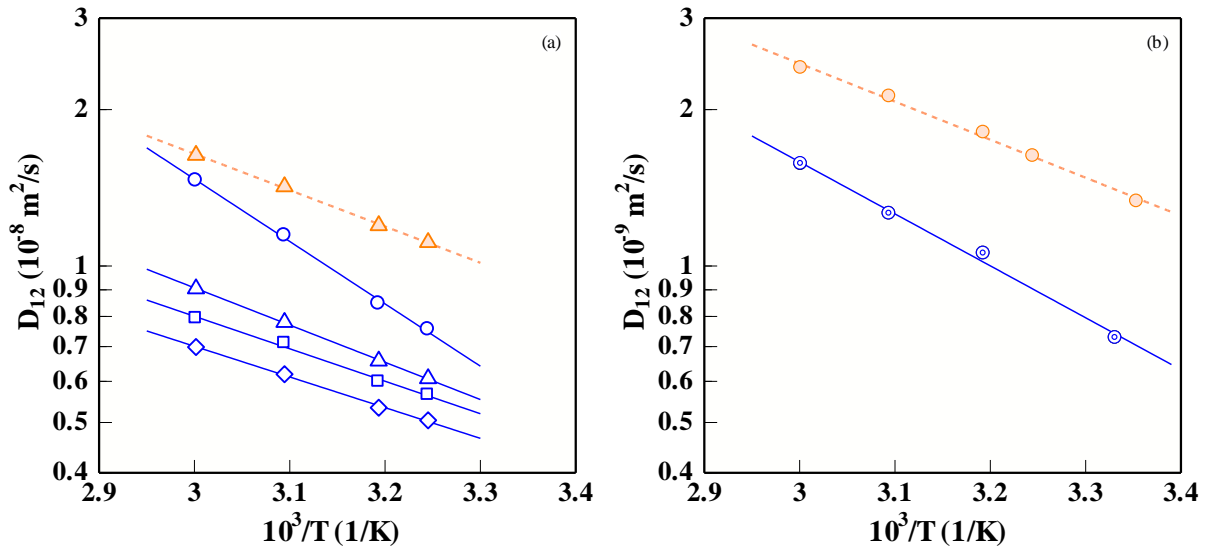
134

Table 2

Correlated results using Eq. (4) for the determined D_{12} values of $\text{Al}(\text{acac})_3$ in supercritical CO_2 .

T (K)	Rang of P (MPa)	N	$c_0 \times 10^9$ (m^2/s)	$c_1 \times 10^7$ ($\text{m}^2 \text{MPa}/\text{s}$)	$c_2 \times 10^{11}$ ($\text{m}^2/(\text{s K})$)	$c_3 \times 10^9$ ($\text{m}^2 \text{MPa}/(\text{s K})$)	AARD (%)
308.15	Entire	29	3.458	0.535	-	-	3.0
	>8.4	22	3.563	0.497	-	-	2.0
313.15	Entire	27	3.184	0.700	-	-	5.3
	>9.5	18	3.503	0.617	-	-	1.5
323.15	Entire	17	3.095	1.002	-	-	3.5
	>12	9	3.768	0.834	-	-	1.6
333.15	Entire	11	2.593	1.333	-	-	2.6
	>14	9	3.491	1.169	-	-	1.8
Common	Entire	84	7.957	-8.476	-1.502	2.929	3.9

135



136

137 Fig. 2. Arrhenius relationship for the diffusion coefficients of $\text{Al}(\text{acac})_3$ in (a) supercritical
 138 CO_2 at 12.00 (\circ), 20.00 (\triangle), 25.00 (\square), 35.00 (\diamond) MPa and (b) liquid ethanol at 0.10 MPa (\odot),
 139 together with those of $\text{Li}(\text{acac})_3$ in the literature [17] at 20.00 MPa (\triangle) in supercritical CO_2 and
 140 at 0.10 MPa (\odot) in liquid ethanol, respectively.

141

142

143 The effects of temperature on D_{12} values of $\text{Al}(\text{acac})_3$ in supercritical CO_2 determined by
 144 the CIR method at 308.15 to 333.15 K and at 12.00, 20.00, 25.00, 35.00 MPa, and in ethanol
 145 determined by the Taylor dispersion method at 300.15 to 333.15 K and 0.10 MPa are plotted
 146 in Fig. 2 along with the $\text{Li}(\text{acac})_3$ data [17] in supercritical CO_2 at 20.00 MPa and in ethanol at
 147 0.10 MPa. A straight line was formed in all plots for each of the pressure investigated. The
 148 D_{12} values can be described using the Arrhenius expression in Eq.(6), where D_0 is the
 149 preexponential factor, E_a is the activation energy, T is the absolute temperature and R the
 150 universal gas constant.

$$151 \quad D_{12} = D_0 \cdot e^{-\frac{E_a}{RT}} \quad (6)$$

152

153

154 In Fig. 2(a), the slope behavior at 12.00 MPa in supercritical CO₂ was distinctly separated
 155 from those at 20.00, 25.00 and 35.00 MPa. The slopes of these lines, however, were different,
 156 indicated different activation energies of diffusion at different pressures. At 20.00 MPa, the
 157 slopes in the plots for Al(acac)₃ and Li(acac) in supercritical CO₂ appeared to be no
 158 significant differences, however, there were considerable differences between the D_{12} values.
 159 Similar behavior can be seen in liquid ethanol as shown in Fig. 2 (b). From the slopes of the
 160 lines in Figs 2 (a) and (b), the activation energies of diffusion for Al(acac)₃ in supercritical
 161 CO₂ and in liquid ethanol were determined. The achieved E_a values of Al(acac)₃ were listed in
 162 Table 3 as well as Li(acac) [17]. The results showed that the activation energies of the
 163 diffusion for Al(acac)₃ were 13.7 and 19.1 kJ/mol at 20.00 MPa in supercritical CO₂ and at
 164 0.10 MPa in liquid ethanol, respectively. These values were slightly higher than those for
 165 Li(acac) under the same conditions [17]. And the determined activation energy values for
 166 Al(acac)₃ in supercritical CO₂ were higher at lower pressures, indicating that diffusion
 167 behavior tended to be more temperature sensitive at lower pressures than it was at higher
 168 pressures.

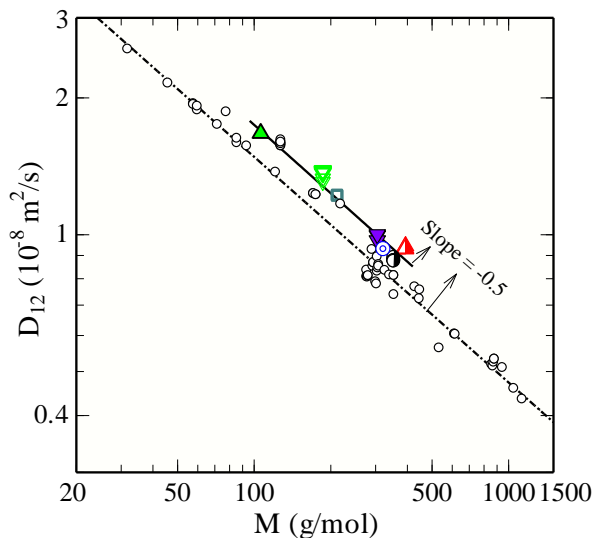
169
170

Table 3.

The values of the activation energy E_a for diffusion in supercritical CO₂ and in liquid ethanol.

Fluid	Solute	E_a (kJ/mol)				
		0.10 (MPa)	12.00 (MPa)	20.00 (MPa)	25.00 (MPa)	35.00 (MPa)
Supercritical CO ₂	Al(acac) ₃		23.0	13.7	12.0	11.3
	Li(acac)			13.4 ^a		
Liquid ethanol	Al(acac) ₃	19.1				
	Li(acac)	14.0 ^a				

^aReported E_a value of Li(acac) in the literature [17].



172

173 Fig. 3. Relationship between the D_{12} data at 313.2 K and 11.0 MPa in supercritical CO_2 and
 174 molecular weight M of $\text{Al}(\text{acac})_3$ (\circ , $M=324.3$ g/mol), together with the other metallic
 175 complexes such as $\text{Li}(\text{acac})$ (\blacktriangle , $M=106.1$ g/mol) [17], ferrocene (\blacktriangledown , $M=186.0$ g/mol) [15],
 176 1,1'-dimethylferrocene (\square , $M=214.1$ g/mol) [15], $\text{Pd}(\text{acac})_2$ (\blacktriangledown , $M=304.6$ g/mol) [14],
 177 $\text{Co}(\text{acac})_3$ (\circ , $M=356.3$ g/mol) [14], $\text{Pt}(\text{acac})_2$ (\blacktriangle , $M=393.3$ g/mol) [16], and the organic
 178 compounds of nonmetallic elements (\circ , $M=32.0 - 1137.9$ g/mol) [21].

179

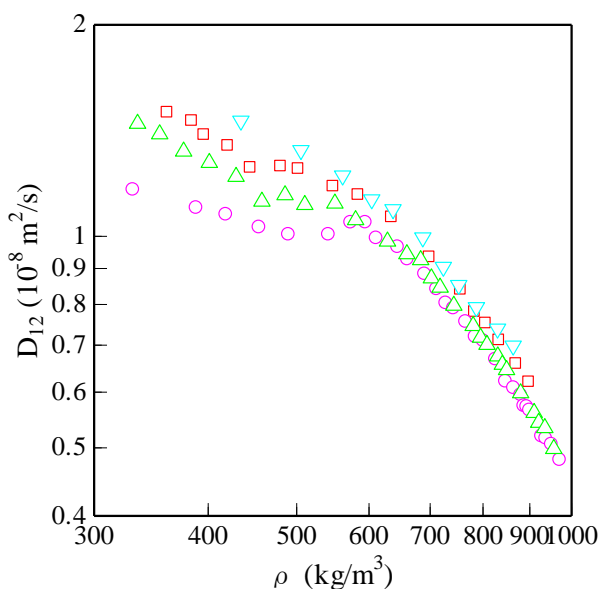
180

181 Fig. 3 plots the D_{12} values measured in this study and reported in literature [14-17, 21] at
 182 313.15 K and 11.00 MPa in supercritical CO_2 against the solute molecular weights M for
 183 various compounds. Overall, a strong dependence of the D_{12} on the solute molecular weight
 184 was found for molecules diffusing within supercritical CO_2 . The D_{12} data of $\text{Al}(\text{acac})_3$
 185 ($M=324.3$ g/mol) measured in this study and literature for other metallic complexes such as
 186 $\text{Li}(\text{acac})$ ($M=106.1$ g/mol) [17], ferrocene ($M=186.0$ g/mol) [15], 1,1'-dimethylferrocene
 187 ($M=214.1$ g/mol) [15], $\text{Pd}(\text{acac})_2$ ($M=304.6$ g/mol) [14], $\text{Co}(\text{acac})_3$ ($M=356.3$ g/mol) [14],
 188 $\text{Pt}(\text{acac})_2$ ($M=393.3$ g/mol) [16] in supercritical CO_2 seemed to be inversely proportional to

189 their molecular weights at constant temperature and pressure with a slope of about -0.5 .
 190 Similar behavior has been observed in the literature [21] for organic compounds of
 191 nonmetallic elements. In addition, most of the D_{12} values of organic compounds of
 192 nonmetallic elements ($M=32.0 - 1137.9$ g/mol) in the literature [21] were lower than those of
 193 metallic complexes ($M=106.1 - 393.3$ g/mol) at the same molecular weights. This result
 194 suggested that the apparent radiuses of metallic complexes appeared to be smaller than those
 195 of organic compounds of nonmetallic elements in supercritical CO_2 . Furthermore, it was also
 196 observed that the D_{12} value of $\text{Pt}(\text{acac})_2$ ($D_{12}=9.350\times 10^{-9}$ m²/s) [16] with M of 393.3 g/mol
 197 had slightly larger value to $\text{Al}(\text{acac})_3$ ($D_{12}=9.250\times 10^{-9}$ m²/s) with M of 324.3 g/mol at 313.15
 198 K and 11.00 MPa in supercritical CO_2 . It may be considered that the apparent molecular size
 199 of $\text{Pt}(\text{acac})_2$ with two acac ligands in supercritical CO_2 exhibited lower value than that of
 200 $\text{Al}(\text{acac})_3$ with three, and in this case the D_{12} value depended not on solute molecular weight.

201

202



203

204 Fig. 4. Density dependence of D_{12} of $\text{Al}(\text{acac})_3$ in supercritical CO_2 at 308.15 K (\circ), 313.15

205 K (\triangle), 323.15 K (\square) and 333.15 K (∇) measured by the CIR method in this study.

206 Fig. 4 shows the D_{12} vs CO_2 density ρ for $\text{Al}(\text{acac})_3$ in supercritical CO_2 . The plots
207 pointed significant temperature dependence over the region of lower density, but those in the
208 higher density region slightly do. In addition, in the CO_2 density region higher than about 580
209 kg/m^3 , the D_{12} values can be linearly correlated with the density at each temperature, but the
210 D_{12} values expressed slowing down in the region of lower density. This slowing down
211 behavior was found clearly as the critical point of CO_2 (31.1 °C, 7.38 MPa) was approached.
212 The behavior of diffusion in the critical region is important to understanding transport
213 phenomena in supercritical fluids. So far, many compounds such as acetone [22], alkane [22],
214 benzene [22, 23], 15-crown-5 [21], dimethylnaphthalene isomers [24], ferrocene [15],
215 myristoleic acid methyl ester [25], naphthalene [24], phenylbutazone [20] and vitamin K_3 [26]
216 have been observed the similar slowing down. But, Yang et al [27] reported that the D_{12} data
217 of benzoic acid, biphenyl, 1,4-dichlorobenzene, phenanthrene and phenol in supercritical CO_2
218 diminished sharply near the critical point. According to Clifford and Coleby [28], the
219 diffusion coefficients for a solute in a supercritical fluid did not show any significant
220 anomalous behavior in the critical region, if the solute concentration was sufficiently low.

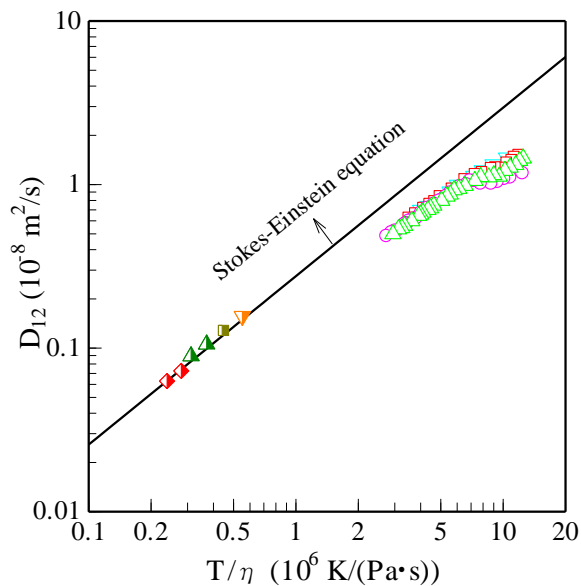
221 The measured D_{12} data of $\text{Al}(\text{acac})_3$ at 308.15, 313.15, 323.15 and 333.15 K in
222 supercritical CO_2 and at 300.15, 313.15, 323.15 and 333.15 K in liquid ethanol as a function
223 of T/η is shown in Fig. 5 with the solid line representing Eq. (7).

$$224 \quad D_{12} = \frac{R}{6\pi r} \frac{T}{\eta} \quad (7)$$

225 where R is the universal gas constant, r is the radius of the diffusing solute and η is fluid
226 viscosity. In this study the diffusion data measured in supercritical CO_2 (with higher T/η
227 values) indicated one order of magnitude larger value than those determined in liquid ethanol
228 (with lower T/η values). The plot in liquid state showed a linear relationship with the slope of
229 1, obviously the well-known Stokes-Einstein equation held good under the liquid condition,

230 but it did not hold well under the conditions including the supercritical state. This indicated
 231 that the apparent molecular diameter of the $\text{Al}(\text{acac})_3$ was led to decrease with increasing
 232 viscosity. As a result, the Stokes-Einstein equation was inadequate to describe the diffusion in
 233 supercritical system.

234



235

236 Fig. 5. Plot of D_{12} vs. T/η for all the D_{12} values measured by the CIR method at 308.15 K
 237 (\circ), 313.15 K (\triangle), 323.15 K (\square) and 333.15 K (∇) in supercritical CO_2 , and measured by the
 238 Taylor dispersion method at 300.15 K (\diamond), 313.15 K (\triangle), 323.15 K (\square) and 333.15 K (∇) in
 239 liquid ethanol. The solid line was obtained from the Eq. (7).

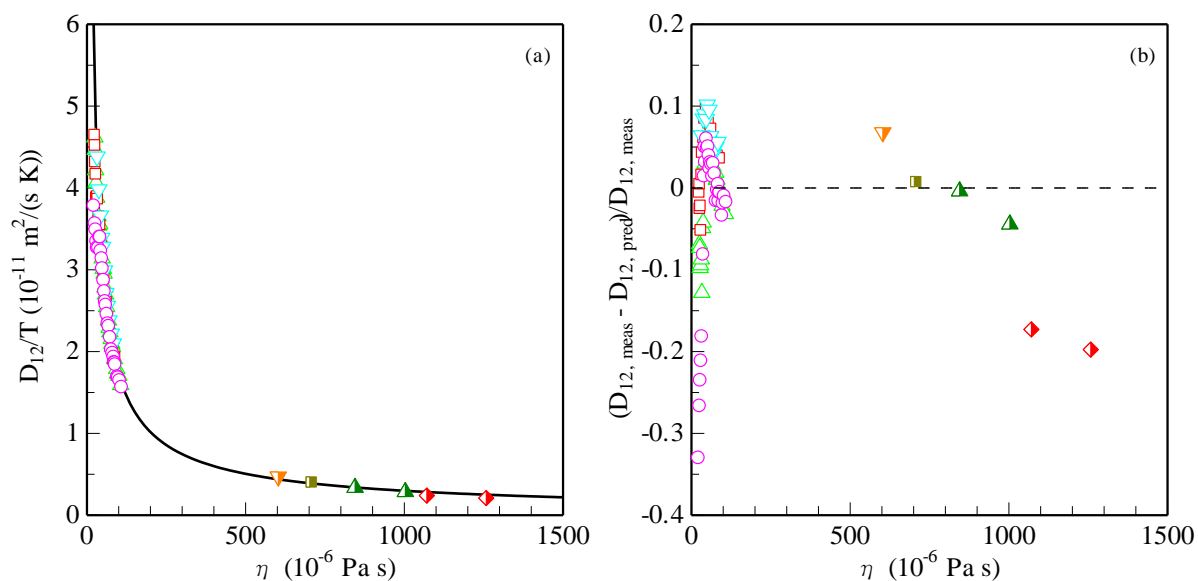
240

241

242 On the hydrodynamic approach for predicting D_{12} in fluids, we have demonstrated
 243 [2,4,5,13-17,20,21,23,25] the validity of the correlation among the properties of D_{12} , T and η ,
 244 as shown in Eq. (8). Fig. 6 indicates D_{12}/T vs η for all the D_{12} data of $\text{Al}(\text{acac})_3$ measured in
 245 this study, together with deviations between the $D_{12, \text{meas}}$ and the $D_{12, \text{pred}}$ values by Eq. (8).

$$246 \quad \frac{D_{12}}{T} = \alpha \eta^\beta \quad (8)$$

247



248
 249 Fig. 6. Plots of (a) D_{12}/T and (b) $(D_{12, \text{meas}} - D_{12, \text{pred}})/D_{12, \text{meas}}$ vs. η for all the D_{12} values
 250 measured by the CIR method at 308.15, 313.15, 323.15 and 333.15 K in supercritical CO_2 , and
 251 measured by the Taylor dispersion method at 300.15, 313.15, 323.15 and 333.15 K in liquid
 252 ethanol. The solid line in (a) was obtained with the parameters of $\alpha=1.558 \times 10^{-14}$ and $\beta=-0.761$
 253 using the Eq. (8). The key is the same as in Fig. 5.

254
 255
 256 where α and β are constants. As has been seen for many compounds, the D_{12}/T values
 257 decrease simply with increasing fluid viscosities. It was found that the values of D_{12}/T for all
 258 D_{12} data of $\text{Al}(\text{acac})_3$ measured in this study were also well correlated with the η values of
 259 fluids, which viscosities were varied over a wide range of values from 2.462×10^{-5} to
 260 1.258×10^{-3} Pa s. And most of the deviation values of $(D_{12, \text{meas}} - D_{12, \text{pred}})/D_{12, \text{meas}}$ were less
 261 than ± 0.2 as seen in Fig. 6 (b). The proposed correlation of $D_{12} [\text{m}^2/\text{s}] = 1.558 \times 10^{-14} T [\text{K}] \eta$
 262 $[\text{Pa s}]^{-0.761}$ can represent the measured 90 D_{12} data in this work with 5.6% AARD values for
 263 the two studied systems of $\text{Al}(\text{acac})_3$ in supercritical CO_2 and $\text{Al}(\text{acac})_3$ in liquid ethanol.

264
 265

266 **5. Conclusions**

267 The infinite dilution binary diffusion coefficients D_{12} for aluminum acetylacetonate were
268 determined by the CIR method in supercritical CO₂ at 308.15, 313.15, 323.15 and 333.15 K
269 and 7.80 to 40.00 MPa. Furthermore, the D_{12} data in liquid ethanol at 300.15, 313.15, 323.15
270 and 333.15 K and at 0.10 and 30.00 MPa were obtained by the Taylor dispersion method. It
271 was found that the D_{12} values measured in supercritical CO₂ show slowing down in the near
272 critical region. The determined activation energies of diffusion were 23.0, 13.7, 12.0, 11.3
273 kJ/mol at 12.00, 20.00, 25.00, 35.00 MPa in the temperature range of 308.15 – 333.15 K in
274 supercritical CO₂ and 19.1 kJ/mol at 0.10 MPa in the temperature range of 300.15 – 333.15 K
275 in liquid ethanol, respectively. All D_{12} data for aluminum acetylacetonate determined in
276 supercritical CO₂ and in liquid ethanol were correlated with the equation of D_{12}
277 $[\text{m}^2/\text{s}] = 1.558 \times 10^{-14} T [\text{K}] \eta [\text{Pa s}]^{-0.761}$ over a wide fluid viscosity range from 2.462×10^{-5} to
278 1.258×10^{-3} Pa s and the average absolute relative deviation of the correlation for 90 data
279 points is 5.6%.
280

281 **References**

- 282 [1] K.K. Liong, P.A. Wells, N.R. Foster, *J. Supercrit. Fluids* 4 (1991) 91-108.
- 283 [2] T. Funazukuri, C.Y. Kong, S. Kagei, *J. Chromatogr. A* 1037 (2004) 411-429.
- 284 [3] C.Y. Kong, *J. Chromatograph. Separat. Techniq.* 5 (2014) e127-2.
- 285 [4] T. Funazukuri, C.Y. Kong, N. Murooka, S. Kagei, *Ind. Eng. Chem. Res.* 39 (2000)
- 286 4462-4469.
- 287 [5] C.Y. Kong, T. Funazukuri, S. Kagei, *J. Chromatogr. A* 1035 (2004) 177-193.
- 288 [6] C.Y. Kong, K. Sone, T. Sako, T. Funazukuri, S. Kagei, *Fluid Phase Equilib.* 302 (2011)
- 289 347-353.
- 290 [7] C.Y. Kong, T. Funazukuri, S. Kagei, G. Wang, F. Lu, *J. Chromatogr. A* 1250 (2012)
- 291 141-156.
- 292 [8] H. Wakayama, H. Itahara, N. Tatsuda, S. Inagaki, Y. Fukushima, *Chem. Mater.* 13 (2001)
- 293 2392-2396.
- 294 [9] D. Barua, T. Gougousi, E.D. Young, G.N. Parsons, *Appl. Phys. Lett.* 88 (2006) 092904-3.
- 295 [10] Q. Peng, D. Hojo, K.J. Park, G.N. Parsons, *Thin Solid Films* 516 (2008) 4997-5003.
- 296 [11] A.I. Cooper, *Adv. Mater.* 15 (2003) 1049-1059.
- 297 [12] X. Yang, M.A. Matthews, *J. Chem. Eng. Data* 46 (2001) 588-595.
- 298 [13] M. Toriumi, R. Katooka, K. Yui, T. Funazukuri, C.Y. Kong, S. Kagei, *Fluid Phase Equilib.*
- 299 297 (2010) 62-66.
- 300 [14] C.Y. Kong, Y. Y. Gu, M. Nakamura, T. Funazukuri, S. Kagei, *Fluid Phase Equilib.* 297
- 301 (2010) 162-167. Pd(acac)₂, Co(acac)₃
- 302 [15] C.Y. Kong, M. Nakamura, K. Sone, T. Funazukuri, S. Kagei, *J. Chem. Eng. Data* 55
- 303 (2010) 3095-3100. Ferrocene
- 304 [16] C.Y. Kong, T. Siratori, G. Wang, T. Sako, T. Funazukuri, *J. Chem. Eng. Data* 58 (2013)
- 305 2919-2924. Pt(acac)₂

- 306 [17] C.Y. Kong, Y. Yakumaru, T. Funazukuri, J. Supercrit. Fluids 104 (2015) 265-271.
307 Li(acac)
- 308 [18] A. Alizadeh, C.A. Nieto de Castro, W.A. Wakeham, Int. J. Thermophys. 1 (1980)
309 243-284.
- 310 [19] T. Funazukuri, C.Y. Kong, S. Kagei, Chem. Eng. Sci. 59 (2004) 3029-3036.
- 311 [20] C.Y. Kong, K. Watanabe, T. Funazukuri, J. Chromatogr. A 1279 (2013) 92-97.
- 312 [21] C.Y. Kong, N. Takahashi, T. Funazukuri, S. Kagei, Fluid Phase Equilib. 257 (2007)
313 223-227.
- 314 [22] S. Umezawa, A. Nagashima, J. Supercrit. Fluids 5 (1992) 242-250.
- 315 [23] T. Funazukuri, C.Y. Kong, S. Kagei, Int. J. Thermophys. 22 (2001) 1643-1660.
- 316 [24] H. Higashi, Y. Iwai, Y. Nakamura, S. Yamamoto, Y. Arai, Fluid Phase Equilib. 166 (1999)
317 101-110.
- 318 [25] C.Y. Kong, M. Mori, T. Funazukuri, S. Kagei, Anal. Sci. 22 (2006) 1431-1436.
- 319 [26] C.Y. Kong, T. Funazukuri, J. Supercrit. Fluids 44 (2008) 294-300.
- 320 [27] X.N. Yang, L.A.F. Coelho, M.A. Matthews, Ind. Eng. Chem. Res. 39 (2000) 3059-3068.
- 321 [28] A.A. Clifford, S.E. Coleby, Proc. R. Soc. Lond. A 433 (1991) 63-79.
- 322

323 Figure Captions

324 Fig. 1. Pressure dependence on the (a) D_{12} and (b) ε of $\text{Al}(\text{acac})_3$ measured at 308.15 K (\circ),
325 313.15 K (\triangle), 323.15 K (\square) and 333.15 K (∇), and at 7.80 to 40.00 MPa in
326 supercritical CO_2 by the CIR method, and together with the correlated line (with best
327 AARD%) by Eq. (4).

328 Fig. 2. Arrhenius relationship for the diffusion coefficients of $\text{Al}(\text{acac})_3$ in (a) supercritical
329 CO_2 at 12.00 (\circ), 20.00 (\triangle), 25.00 (\square), 35.00 (\diamond) MPa and (b) liquid ethanol at 0.10
330 MPa (\odot), together with those of $\text{Li}(\text{acac})$ in the literature [17] at 20.00 MPa (\triangle) in
331 supercritical CO_2 and at 0.10 MPa (\circ) in liquid ethanol, respectively.

332 Fig. 3. Relationship between the D_{12} data at 313.2 K and 11.0 MPa in supercritical CO_2 and
333 molecular weight M of $\text{Al}(\text{acac})_3$ (\odot , $M=324.3$ g/mol), together with the other metallic
334 complexes such as $\text{Li}(\text{acac})$ (\blacktriangle , $M=106.1$ g/mol) [17], ferrocene (\blacktriangledown , $M=186.0$ g/mol)
335 [15], 1,1'-dimethylferrocene (\square , $M=214.1$ g/mol) [15], $\text{Pd}(\text{acac})_2$ (\blacktriangledown , $M=304.6$ g/mol)
336 [14], $\text{Co}(\text{acac})_3$ (\circ , $M=356.3$ g/mol) [14], $\text{Pt}(\text{acac})_2$ (\blacktriangle , $M=393.3$ g/mol) [16], and the
337 organic compounds of nonmetallic elements (\circ , $M=32.0 - 1137.9$ g/mol) [21].

338 Fig. 4. Density dependence of D_{12} of $\text{Al}(\text{acac})_3$ in supercritical CO_2 at 308.15, 313.15, 323.15
339 and 333.15 K measured by the CIR method in this study. The key is the same as in Fig.
340 1.

341 Fig. 5. Plot of D_{12} vs. T/η for all the D_{12} values measured by the CIR method at 308.15 K (\circ),
342 313.15 K (\triangle), 323.15 K (\square) and 333.15 K (∇) in supercritical CO_2 , and measured by
343 the Taylor dispersion method at 300.15 K (\blacklozenge), 313.15 K (\blacktriangle), 323.15 K (\blacksquare) and
344 333.15 K (\blacktriangledown) in liquid ethanol. The solid line was obtained from the Eq. (7).

345 Fig. 6. Plots of (a) D_{12}/T and (b) $(D_{12, \text{meas}} - D_{12, \text{pred}})/D_{12, \text{meas}}$ vs. η for all the D_{12} values
346 measured by the CIR method at 308.15, 313.15, 323.15 and 333.15 K in supercritical
347 CO_2 , and measured by the Taylor dispersion method at 300.15, 313.15, 323.15 and
348 333.15 K in liquid ethanol. The solid line in (a) was obtained with the parameters of
349 $\alpha=1.558 \times 10^{-14}$ and $\beta=-0.761$ using the Eq. (8). The key is the same as in Fig. 5.

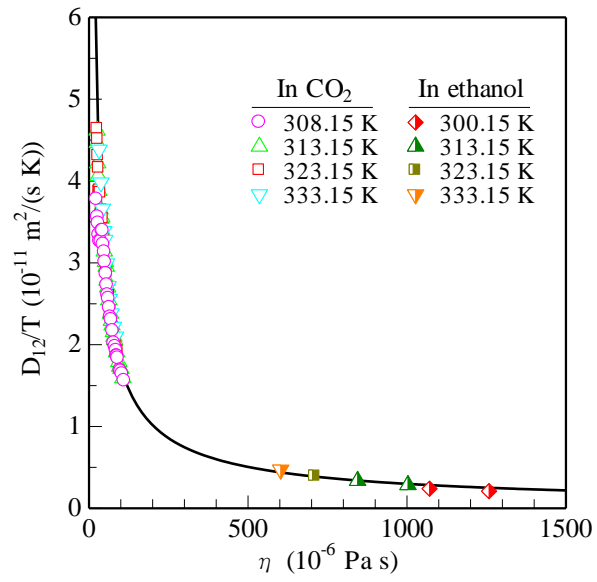
350

351

352

353 Graphical abstract

354



355